NRC Research Press

ARTICLE

Spatial and temporal quantification of forest residue volumes and delivered costs

Lucas A. Wells, Woodam Chung, Nathaniel M. Anderson, and John S. Hogland

Abstract: Growing demand for bioenergy, biofuels, and bioproducts has increased interests in the utilization of biomass residues from forest treatments as feedstock. In areas with limited history of industrial biomass utilization, uncertainties in the quantity, distribution, and cost of biomass production and logistics can hinder the development of new bio-based industries. This paper introduces a new methodology to quantify and spatially describe delivered feedstock volumes and costs across landscapes of arbitrary size in ways that characterize operational and annual management decision-making. Using National Agricultural Imagery Program (NAIP) imagery, the forest is segmented into operational-level treatment units. A remote sensing model based on NAIP imagery and Forest Inventory and Analysis plot data are used to attribute treatment units with stand-level estimates of basal area, tree density, aboveground biomass, and quadratic mean diameter. These methods are applied to a study site in southwestern Colorado to assess the quantity and distribution of treatment residue for use in bioenergy production. Results from the case study demonstrate how this generalized approach can be used in the analysis and decision-making process when establishing new bioenergy industries that use forest residue as feedstock.

Key words: forest biomass, stand characteristics, treatment residue, bioenergy, stand delineation.

Résumé : La demande grandissante pour la bioénergie, les biocarburants et les bioproduits a augmenté l'attrait pour l'utilisation comme matière première de la biomasse résiduelle générée par les traitements sylvicoles. Dans les régions qui ont une expérience limitée de l'utilisation industrielle de la biomasse, les incertitudes concernant la quantité, la distribution ainsi que le coût de production et la logistique de la biomasse peuvent nuire au développement de nouvelles bio-industries. Cet article présente une nouvelle méthodologie pour quantifier et décrire spatialement les volumes et les coûts de la matière première livrée dans un paysage aux dimensions arbitraires et d'une façon qui caractérise le processus de prise de décision opérationnelle et annuelle d'aménagement. À l'aide des images du Programme national d'imagerie agricole (NAIP), la forêt a été segmentée en unités de traitement sur la base des contraintes spatiales définies par les utilisateurs. Un modèle de télédétection fondé sur les images du NAIP et sur les données des places échantillons du Programme d'analyse et d'inventaire forestiers est utilisé pour attribuer les unités de traitement avec des estimations à l'échelle du peuplement de la surface terrière, de la densité des arbres, de la biomasse aérienne et du diamètre de la tige de surface terrière moyenne. Ces méthodes sont appliquées à une station expérimentale dans le sud-ouest du Colorado pour évaluer la quantité et la distribution des résidus de traitement pour la production de bioénergie. Les résultats de cette étude de cas démontrent comment cette approche généralisée peut être utilisée dans le processus d'analyse et de prise de décision lors de l'établissement de nouvelles industries bioénergétiques qui utilisent les résidus de la forêt comme matière première. [Traduit par la Rédaction]

Mots-clés : biomasse forestière, caractéristiques des peuplements, résidus de traitement, bioénergie, délimitation des peuplements.

1. Introduction

The interior western United States (US) has experienced growing interest in using forest biomass as a renewable source of energy. Historically, the use of forest biomass has been dominated by the forest products industry for generating heat, steam, and electricity (Guo et al. 2007). However, emerging markets for forest biomass as a fuel and feedstock for bioenergy applications can be found throughout the US. In the western US, interests in these potential and emerging markets are closely linked to the increasing risk of significant forest disturbances such as fire, insects, and disease and by the broad agreement that silviculture using active treatments, including thinning and prescribed fire, is urgently needed to restore historic stand dynamics and improve forest health (Brown et al. 2004). The large potential treatment area throughout the western US presents opportunities to increase the use of renewable energy sources and stimulate local economic development with new bioenergy and bio-based product enterprises that will use the woody biomass by-products produced by these treatments.

In the 15 western states of the US, there are at least 11 million hectares (ha) that could benefit from some type of treatment to restore ecosystems, protect water and soil quality, and improve forest and rangeland resilience (Rummer et al. 2003). Assuming that such management occurs only on forests with annual timber production of at least 21 $m^3 \cdot ha^{-1}$, an estimated biomass availability of

Received 9 November 2015. Accepted 1 April 2016.

L.A. Wells.* Department of Forest Management, University of Montana, 32 Campus Way, Missoula, MT 59801, USA.
W. Chung. Department of Forest Engineering, Resources and Management, Oregon State University, 276 Peavy Hall, Corvallis, OR 97331, USA.
N.M. Anderson and J.S. Hogland. Rocky Mountain Research Station, USDA Forest Service, 800 East Beckwith, Missoula, MT 59801, USA.
Corresponding author: Woodam Chung (email: woodam.chung@oregonstate.edu).
*Present address: Department of Forest Engineering, Resources and Management, Oregon State University, 068 Peavy Hall, Corvallis, OR 97331, USA.

Published at www.nrcresearchpress.com/cjfr on 12 April 2016.

245 million dry tonnes (t) could result from forest treatments on 4.3 million ha in the west (Western Governors' Association, Western Regional Biomass Energy Program; www.westgov.org/wga/initiatives/biomass/). The U.S. Department of Energy and the USDA Forest Service estimated that an annual supply of 907 million t of biomass would displace 30% or more of domestic petroleum consumption. Of this amount, the continental US could potentially produce 429 million t at \$54.43·t^{-1} (currency in US dollars throughout) from forest residue and agricultural waste in 2012 (U.S. Department of Energy 2011).

Recent studies have evaluated the benefits associated with the use of treatment residues for bioenergy production. Gan and Smith (2007) found that removing logging residues would save \$495–\$620·ha^{-1} in site preparation costs during forest regeneration in East Texas. Results from Jones et al. (2010) show that bioenergy, as an alternative to on-site burning, generates fewer carbon dioxide (CO_2), methane (CH_4), and particulate matter (PM) emissions. Loeffler and Anderson (2014) examined emissions from co-firing forest biomass with coal and found that at 20% substitution, or 120 717 t of forest biomass per year, total system emissions decreased 15% for CO_2, 95% for CH_4, 18% for nitrogen oxides (NO_x), 82% for PM_{10}, and 27% for sulfur oxides (SO_x). Furthermore, there could be economic benefits in using revenues from biomass to offset restorative treatment costs (Brown et al. 2004).

The availability of biomass at tactical and operational scales relies on many factors such as current biomass stocks, harvesting systems, terrain, road network, species, forest characteristics, silviculture, ownership, public policy and regulation, local markets, and management objectives, yet these factors are often ignored in large-scale forest biomass supply models that focus on biomass stocks. This is largely attributable to the complexity of forest landscapes and the difficultly in modeling spatial and temporal details of forest management activities. There is a need for an integrated framework to provide realistic forest biomass supply and costs of feedstock across a large landscape at a tactical resolution that takes into account forest inventory, existing infrastructure, and current forest management objectives applied across multiple scales and time frames. A standardized approach for carrying out such an assessment does not exist and likely is not possible given the variability in forests, management practices, and policies across the western US. Nonetheless, a workflow to guide these types of assessments and tools to help decision-makers quantify and spatially describe treatment residue supply volumes is needed to accompany a growing bioenergy enterprise. Broadly, providing high-resolution estimates of biomass stocks and potential flows from restoration treatments at spatial and temporal scales that are relevant to the industry is critical for facility capitalization, construction, and planning. Operationally, in the context of meeting nonmarket forest restoration objectives, managers can identify and prioritize treatments with costs that are well matched with both overall demand and the market price of biomass. The overall effect of offsetting the costs of restoration treatments with revenues from both timber and biomass would be to allow forest managers to treat more acres at lower cost.

The objectives of this study are to (*i*) develop a generalized workflow to evaluate forest biomass utilization and bioenergy supply at tactical and operational scales through space and time and (*ii*) demonstrate the utility of the proposed methodology via application to a study area in southwestern Colorado.

2. Methods

The central components of the presented methodology and their role in the workflow are highlighted in Fig. 1. The workflow consists of three process modules: stand characterization, treatment simulation, and feedstock cost estimation. In the first module, we use modern remote sensing and image processing techniques to produce forest stand boundaries and stand descriptive statistics.

Fig. 1. Overview of the workflow components for estimating treatment residue quantity, spatial distribution, and delivered costs.

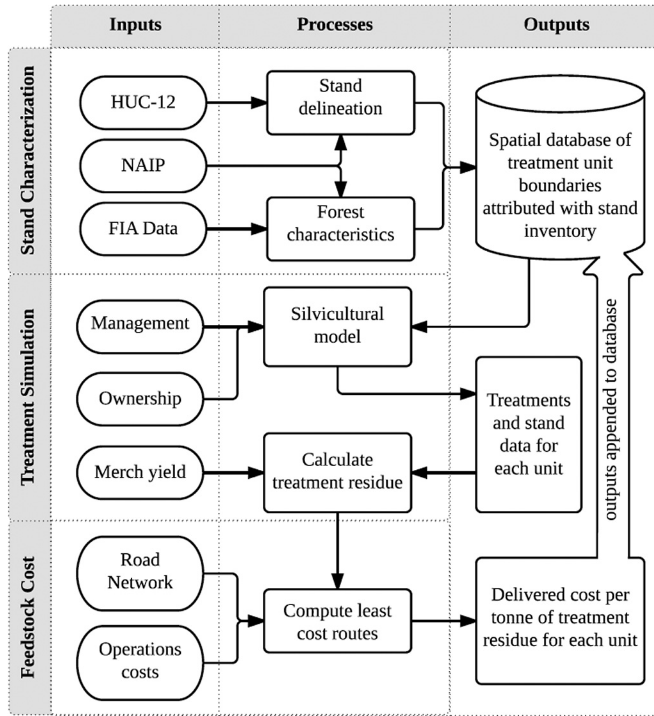

These outputs are then coupled with site-specific silvicultural prescriptions in the second module to estimate retention, merchantable yield, and resulting recoverable biomass residue volumes. The third module routes the recoverable biomass volumes to a conversion facility by least-cost route and estimates delivered costs of feedstock. Because it is difficult to describe some of the methods in the absence of a site-specific example, we present the generalized, non-site-specific methods (i.e., stand characterization module) in the following section and then present the subsequent modules in sections 2.2 and 2.3 after introducing the case study area and site-specific data.

2.1. Stand characterization module

2.1.1. Imagery

Imagery of the National Agricultural Imagery Program (NAIP) was used to estimate forest characteristics and define potential treatment units. NAIP acquires aerial digital orthophotos during the agricultural growing seasons and the imagery is publicly available within a year of acquisition. The imagery has a 1 m ground sample distance (1 m spatial resolution) with a horizontal accuracy of within 6 m at a 95% confidence level (USDA Farm Service Agency, NAIP; http://www.fsa.usda.gov/programs-and-services/aerial-photography/imagery-programs/naip-imagery/) and a temporal resolution of 2 to 5 years. The default spectral resolution is natural color (RGB) with an option to include the near-infrared band. The configuration used in this study was a three-band composite including near-infrared, green, and blue bands (color-infrared imagery, CIR).

2.1.2. Stand delineation

An automated forest segmentation algorithm (Wells 2013), hereinafter referred to as the stand delineation algorithm (SDA), was developed in this study to delineate forest landscapes into operational-level treatment units. The SDA employs a series of image-filtering techniques and the mean-shift algorithm (Fukunaga and Hostetler 1975) to decompose NAIP imagery into individual forest stands defined as "a contiguous group of trees sufficiently

Fig. 2. Flowchart of the stand delineation algorithm.

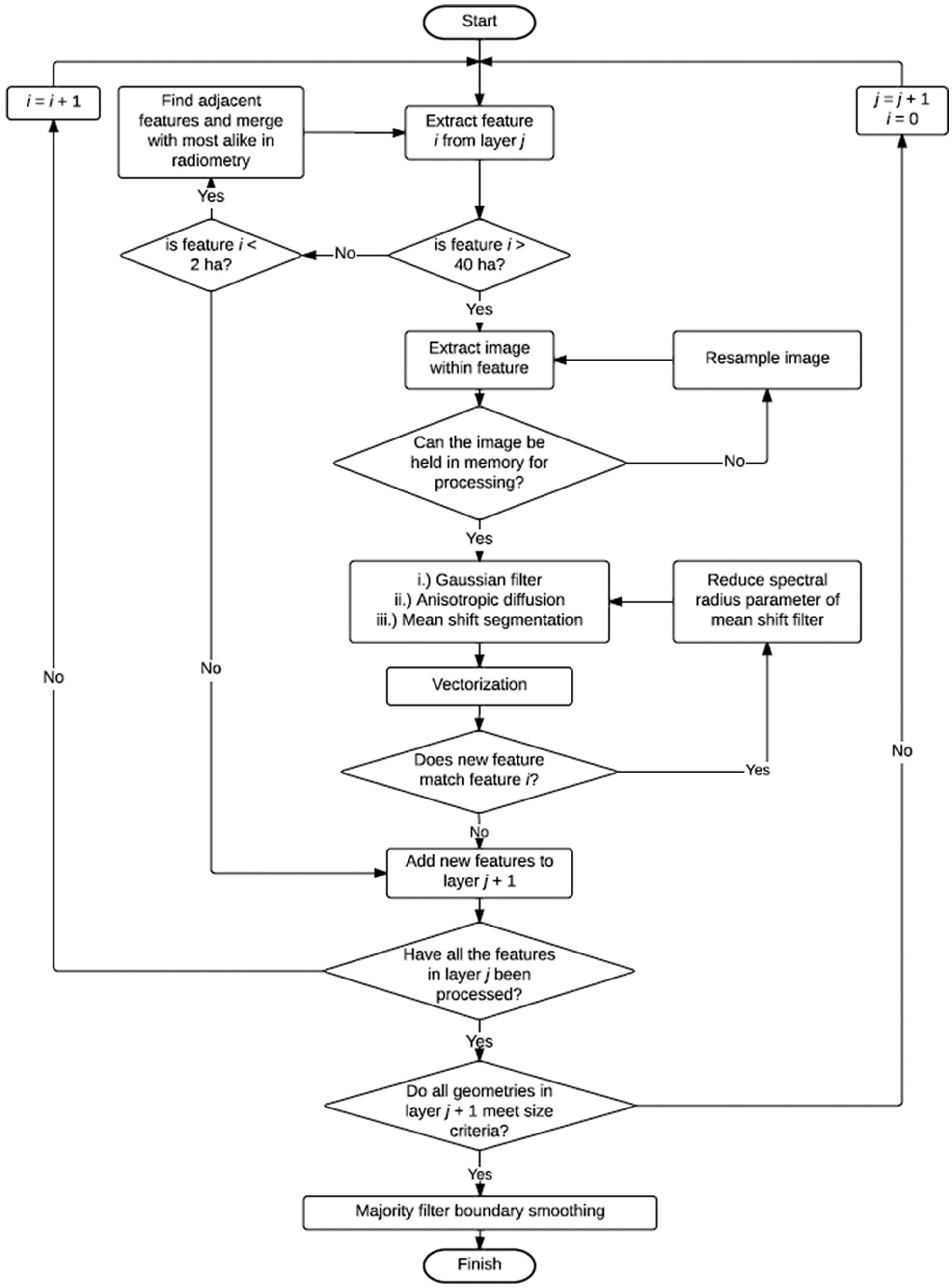

uniform in age-class distribution, composition and structure, and grown on a site of sufficiently uniform quality to be a distinguishable unit" (Helms 1998). These processes are embedded in a subspace, multiscale framework to circumvent computational limitations associated with large scenes of very high resolution imagery. The algorithm uses 12-digit hydrological unit (U.S. Geological Survey (USGS) 2006) boundaries, also called subwatersheds, as initial subspace geometries. New geometries created by the segmentation process within each subwatershed are stored in a vector database and used to further subset the image in the next iteration. As objects become smaller, finer resolutions are used for segmentation to locate features that may not be visible at coarser scales. The algorithm can also be parameterized to comply with minimum and maximum treatment unit area constraints. Minimum and maximum treatment unit area constraints were 2 and 40 ha, respectively.

The algorithm begins by querying geometry i from database j (Fig. 2). If geometry i is less than the maximum specified treatment unit size and greater than the minimum specified treatment unit size, then the geometry is not segmented further. It is appended to vector database $j + 1$ and the algorithm moves to the next geometry $i + 1$. If the geometry is less than the minimum specified treatment unit size, then adjacent geometries are located and geometry i is merged with the candidate adjacent geometry most alike in terms of the mean spectral value. If geometry i is greater than the maximum specified treatment unit size, then the imagery within the geometry is extracted for segmentation.

The next step tests if the extracted image results in memory saturation. If the image is too large, it is resampled by iteratively decreasing the resolution (i.e., 1 m, 2 m, 4 m, 8 m, 16 m, etc.) until the image can be stored in memory. Once the image is sufficiently resampled, it is convolved with a 3 × 3 Gaussian filter (σ = 0.5) and 50 iterations of the anisotropic diffusion filter (time step = 0.125). Next the mean shift algorithm segments the image by clustering cells to their associated local maxima and labels the groups sequentially. The resulting labeled raster is vectorized and appended to database $j + 1$.

In some cases, the new geometry i in database $j + n$ could match geometry i in database $j + (n - 1)$ if the chosen resolution for segmentation is the same resolution at which geometry i in database $j + (n - 1)$ was processed. If this occurs, the spectral radius parameter of the mean shift algorithm is iteratively reduced by one until new geometries are created. Reducing this parameter allows the mean shift segmentation to produce more geometries with similar spectral values as opposed to merging these modes as one cluster. When new geometries are created, they are appended to vector database $j + 1$.

Once all geometries in database j have been processed, the algorithm iterates through the geometries in database $j + 1$. When all the geometries in database $j + n$ meet the minimum and maximum unit size criteria, the final vector database is rasterized to a 1 m resolution and the dataset is smoothed. Next the smoothed raster is vectorized and the process is terminated. The hierarchy of spatial vector data is used in Fig. 2, where "layer" describes the database where geometries or "features" are stored.

The resulting stand boundaries were assessed qualitatively by visual evaluation and quantitatively by minimum, maximum, and mean area and shape compactness value. Compactness is a proportional metric between the area of a feature and the area of a circle having the same perimeter of said feature. Compactness was determined to be an important measure from a forest operations perspective due to inefficiencies in elongated (noncompact) areas where the area-to-perimeter ratio is low. The compactness value was calculated by $A_i/\pi\left(\frac{P_i/\pi}{2}\right)^2$, where A_i is the area of the stand and P_i is the perimeter of the stand. Thus, a stand with a compactness value of 1 would be a circle.

2.1.3. Stand characteristics

Stand characteristics, including basal area, tree density, and aboveground biomass, are estimated for each treatment unit using the Forest Characteristics Model (FCM) (Hogland et al. 2014). The FCM is a two-tiered remote sensing model in which the first stage performs a probabilistic classification of identifiable patterns (e.g., tree canopy, shadow, grass, or water) within NAIP imagery. The classification is the result of a polytomous logistic regression scheme (Hogland et al. 2013) employing a collection of texture derivatives as explanatory variables. The classification output and texture derivatives of each class are summarized for the spatial footprint bounding the four subplots of a Forest Inventory and Analysis (FIA) field plot and related to mean plot estimates of basal area, tree density, and aboveground biomass using multivariate linear regression. The result is a multiband raster dataset in which each pixel (1 m^2) represents mean plot estimates of forest characteristics for each species group. Aboveground biomass estimates are derived from equations found in Jenkins et al. (2003) and thus can be used to calculate stump, bole, top, and foliage biomass components. Quadratic mean diameter (QMD, cm) is added to the dataset post hoc by $(BA/[k \times t_d])^{1/2}$, where BA is basal area ($m^2 \cdot ha^{-1}$), t_d is tree density (stems$\cdot$ha^{-1}), and k = 0.00007854 (foresters constant). For model validation methods and results, see Wells (2013).

2.2. Treatment simulation module

The treatment simulation and feedstock cost-estimation modules in this study require site-specific data. To facilitate effective presentation of the two modules, we introduce our case study area and follow with a description of the modules.

2.2.1. Case study area

The study area includes the extent of the Uncompahgre Plateau National Forest (UPNF). The UPNF covers approximately 235 000 ha on the western slope of the Colorado Rocky Mountains. Stretching northwest to southeast for 200 km, the plateau ranges in elevation from 1700 to 1800 m in canyon bottoms to upland elevations around 2500–3000 m. Three primary vegetation strata occupy the plateau. Pinyon–juniper (*Pinus edulis* Engelm., *Juniperus osteosperma* [Torr.] Little, and *Juniperus scopulorum* Sarg.) cover occurs at the lower elevations ranging from 1800 to 2100 m. Gamble oak (*Quercus gambelii* Nutt.) and Ponderosa pine (*Pinus ponderosa* Douglas ex C. Lawson) forests inhabit elevations from 2200 to 2700 m and occur in both mixed and pure stands. The upland zone is dominated by aspen (*Populus tremuloides* Michx.), mixed-conifer, and spruce–fir (*Picea engelmannii* Parry ex Engelm. and *Abies lasiocarpa* [Hook.] Nutt.) forests.

Approximately 70% of the UPNF is in fire regime condition class 2 or 3 (Hardy et al. 2001; Schmidt et al. 2002), suggesting that these areas exhibit fuel conditions that are conducive to uncharacteristic, high-intensity fires. The potential for these disturbance events have initiated active restoration management across the plateau to reduce fuel loading in mixed-conifer and Ponderosa pine, increase diversity in age, size, and seral conditions in spruce–fir, regenerate damaged aspen stands from sudden aspen decline, and mitigate pinyon–juniper encroachment into native grasslands and sagebrush ecosystems.

The renewable energy portfolio standard recently implemented in Colorado has stimulated the need to incorporate a higher level of renewable resources into energy production systems, including wind, solar, and biomass. Co-firing biomass with coal has been explored as an option to meet this standard (Loeffler and Anderson 2014). Though not currently a source of biomass demand, in this study a 100 MW coal-fired electric power plant located approximately 16 km west of the eastern border of the study area served as the hypothetical bioenergy facility. Although this particular power plant is fueled completely by bituminous coal, it could be retrofitted to co-fire forest biomass.

2.2.2. Modeling silvicultural prescriptions and prioritizing stands for treatments

GIS coverage of forest roads on the UPNF was used to query accessible treatment units. These units were defined as having a centroid that fell within maximum skidding distance for whole-tree harvesting from an existing road edge, assumed to be 610 m (2000 feet) in this study. Three quantifiable silvicultural prescriptions were developed to model removal and retention of biomass on candidate treatment units. These prescriptions are generalized and adapted from the current forest plan for the UPNF (USDA Forest Service 2012) and from a management plan assembled by the Uncompahgre Plateau Collaborative Restoration Project (UPCRP). Management planning documents provided detailed information regarding current conditions, including problems with forest health, reference conditions, and desired future conditions. Stands assigned to a silvicultural prescription are a subset of the accessible treatment units and classified as candidate treatment units. Such stands are included in the selection pool as potential treatment units but may or may not receive treatment under a given scenario.

Stands were categorized into species groups based on a basal area weighted species composition. Pure stands were considered to have a composition of at least 80% in a single species. Species groups describing two species were stands with an additive composition of 80% in two species. Mixed-conifer species group distinguishes stands with a composition of at least 80% of any combination of spruce–fir, pine, and aspen. Current treatment prescriptions and associated logging systems (e.g., mechanized thinning with whole-tree skidding) in spruce–fir, mixed-conifer, aspen, and pine stands present opportunities for residue extraction due to the centralization of residues during whole-tree harvesting (above the stump) operations. In contrast, treatments in other species groups such as pinyon–juniper and gamble oak, where mastication, lop-and-scatter, and decentralized pile burning are deployed, have logistical limitations that reduce potential for biomass residue extraction. Specifically, harvest and collection of biomass residues left behind after these types of treatments can be extremely expensive because the materials are spread over large areas rather than centralized. Therefore, only species groups commonly treated with whole-tree skidding are included in this study. These species groups are used to apply a silvicultural prescription to candidate treatment units for the purpose of estimating how much residue will be produced from the activity. These prescriptions include stocking-based, regeneration, and restoration approaches.

Stocking-based management

This study uses stocking-based management prescriptions that reduce stand density for reduction of fuels. This approach is commonly applied to spruce–fir and mixed-conifer forest types in the study area. Stand density index (SDI), introduced by Reineke (1933), was used to develop silvicultural guidelines specific to the selected stands. The maximum SDI was located by plotting tree density against QMD (D_q) for all stands selected for stocking-based management on log–log axes. A line with a slope of –1.605, suggested by Reineke (1933) as the cross-species slope of the 100% stocking line, was hand-fitted on the right edge of the data. Density (trees·ha^{-1}) was then indexed where the 100% stocking line and D_q = 25 cm intersected, resulting in a maximum SDI of 717 trees·ha^{-1}. For the purpose of this analysis, the hand-fitting method was considered sufficient at removing enough subjectivity in locating maximum SDI because the slope of the line was constrained to –1.605. See Zhang et al. (2005) for a comparison of more objective methods for fitting the self-thinning line.

Relative density (RD) was calculated for each stand by dividing SDI by the maximum SDI (717). Stands with RD of ≥60% were considered candidate stands for a treatment during the simulation time frame. The target management zone was bounded by a lower zone at 35% of maximum SDI and an upper zone at 60% of maximum SDI. When a given stand was selected for treatment, it was assumed that the treatment would reduce the stand's SDI to 47.5% (half of the distance between the lower and upper management zones) of the maximum SDI. Stands were prioritized by iteratively selecting the highest RD and then removing the stand from the selection pool. This approach facilitates efficient treatment application by prioritizing the densest stands for treatment.

Regeneration management

Regeneration management was applied to pure aspen stands and aspen stands with a conifer component no greater than 40%. Two important aspects of aspen management across the study area are sudden aspen decline (SAD) and conifer encroachment. The management goal in both situations is to establish a vigorous regenerative age class of aspen. Branch dieback in aspen stands was first noted in southwestern Colorado in 2004 (Worrall et al. 2008) and soon after was dubbed "sudden aspen decline", characterizing the sudden, rapid progression of the disease. To this end, the etiology of SAD has been widely studied and recent assessments suggest that SAD appears to have a strong correlation with climate, and SAD-like events commonly occur earlier in regions with higher temperatures and drier climates (Hogg 1997; Shields and Bockheim 1981).

Results from Worrall et al. (2010) conclude that the areas experiencing the greatest mean moisture deficit during the drought of 2002 showed the highest degree of decline in 2008. This was statistically tested by relating climate moisture index (CMI) values to inventoried aspen stands. Because outputs from the FCM do not provide information regarding mortality, aspen management was prioritized by calculating CMI for the study area and allocating treatments to stands with the highest susceptibility to decline in the event of extreme heat and moisture deficiency.

CMI is an index of moisture surplus or deficit, simply precipitation minus potential evapotranspiration. CMI was calculated using an approach outlined by Hogg (1997). Monthly PRISM climate data (Daly et al. 2009) for 2002 (a year of drought) on a 4 km grid and a digital elevation model with 10 m spatial resolution were obtained covering the extent of the study area. The 2002 annual CMI was determined by summing the monthly CMI values. These values were used to locate susceptible areas during extreme conditions similar to the drought of that year.

Because multiple stands fell within each CMI grid cell, auxiliary information was needed to further prioritize treatments. To augment CMI, the topographic wetness index (TWI) was calculated for the study area using the elevation dataset. Topography affects the spatial distribution of soil moisture, and subsurface flow often follows surface topography (Rodhe and Seibert, 1999; Seibert et al. 1997; Zinko et al. 2005); therefore, this index has been used to depict spatial soil moisture patterns (Burt and Butcher 1986; Moore et al. 1991). TWI provided local information regarding potential stress in aspen stands due to moisture deficit within each 4 km cell of the CMI. TWI was computed by $\ln(a/\tan\beta)$, where a is the local upslope area draining through a certain point per unit contour length and $\tan\beta$ is the local slope (Beven and Kirkby 1979).

Treatments were prioritized first by locating stands with the lowest CMI value, then locating stands with the lowest mean TWI value. When a given stand encountered a treatment event, a regeneration cut was simulated removing 100% of the estimated growing stock and subtracting merchantable yield to estimate the amount of treatment residue.

Restoration in ponderosa pine

Restoration treatments were applied to pure ponderosa pine stands, as well as aspen–pine and juniper–pine stands with a pine component of at least 60%. The majority of ponderosa pine stands across the plateau no longer exhibit the structure that was common in the 19th century (Binkley et al. 2008). Historically, these stands had a clumped distribution, interspersed with small (0.04 to 0.2 ha) meadows and basal area ranging from 5 to 20 m^2·ha^{-1}. Many of the stands on the plateau exceed 20 m^2·ha^{-1} and a few were well over 35 m^2·ha^{-1}. Restoration treatments for ponderosa pine in this study reduced basal area to 5–11 m^2·ha^{-1} following recommendations from Binkley et al. (2008). The basal area of each treated stand was reduced to 8 m^2·ha^{-1}. Treatments were prioritized by iteratively selecting the stand with the highest basal area value and thinning to the target basal area. Treatment residues were calculated by subtracting retention and merchantable yield from aboveground biomass for each treated stand.

2.2.3. Treatment residue volumes

Residue was estimated for each candidate treatment unit by first subtracting the removed biomass from the total aboveground biomass then subtracting gross merchantable yield. The amount of removed biomass was determined by the silvicultural prescription, while the gross merchantable yield was calculated by using a component ratio estimator for stem wood and stem bark based on QMD and tree length from a 30 cm stump height to a 10 cm top diameter (Jenkins et al. 2003). Total treatment residues were reduced by 30% to account for the leakage during transport from stump to landing and the recovery rate of the residue at the landing (Baral and Guha 2004; Fight et al. 2006). These operational constraints also effectively leave a significant amount of woody biomass on the unit to meet guidelines for retention associated with soil and biodiversity objectives (Abbas et al. 2011). Equation 1 was used to calculate treatment residue (TR):

$$\text{TR} = r\left([B_{ag} - B_{sr}][1 - e^{\beta_0 + \frac{\beta_1}{D_q}}]\right) \tag{1}$$

where B_{ag} is aboveground biomass, B_{sr} is silviculturally retained biomass (biomass units in dry tonnes per hectare). β_0 and β_1 are the species-specific component ratio coefficients for stem wood and stem bark, respectively, D_q is the QMD for the stand, and r is the reduction factor of leakage and recovery rates (0.7). Residue extraction was assumed to take place after the removal of the commercial component and residue was allowed time to dry to a moisture content of 30% (Han et al. 2010).

2.3. Feedstock cost-estimation module

The harvesting system for each treatment was assumed to be mechanical felling with a feller–buncher followed by whole-tree skidding in which the tops and limbs of the removed trees were transported with the bole to a roadside landing designated for each unit. The extraction operation was assumed to be roadside processing and biomass grinding because all candidate treatment stands were selected to be within the maximum skidding distance of 610 m to the unit centroid from the existing road network. A marginal cost approach was used to calculate forest operations costs (Puttock 1995). This approach considers biomass to be a by-product of the production of higher value components such as sawlogs and fully allocates harvest costs of felling, extraction, processing, road construction, and stumpage to these products. Therefore, costs begin to accrue with the collection of residues at the roadside. Handling, processing, and loading costs for residues were calculated following methods from Anderson (2011) by averaging the results from 40 scientific studies examining biomass removal from timber harvest, fuel treatments, and other residue-related operations resulting in $31.14·t^{-1}.

Transportation costs (T, \$·t^{-1}) were calculated for each candidate treatment unit:

$$T = \frac{(h + l + u)\left\{c + p + \left(d\left[1 + \frac{a}{100}\right]s^{-1}v\right)\right\}}{m(1 - w)} \tag{2}$$

Optimized round-trip delivery times, denoted by variable h (hours, h) in eq. 2, from each unit to the potential bioenergy facility were calculated using GIS coverage of all UPNF roads. A transportation network optimization program was used to determine the least-cost route for each unit based on engineered road speed (Chung and Sessions 2003). Other variables used to calculate transportation costs were load time (l) and unload time (u), each assumed to be 0.5 h, non-fuel trucking (operator) cost (c) set at \$48.03·h^{-1} (American Transportation Research Institute (ATRI) 2013), a specialized trucking premium (p) of \$12.00·h^{-1}, \$1.04·L^{-1} for diesel fuel price (d) (U.S. Energy Information Administration; http://www.eia.gov/, accessed 2 October 2013), mean fuel economy (s) of 1.98 km·L^{-1}, mean truck speed (v, km·h^{-1}), which depends on the engineered road speed of the shortest path distance for each unit, lubrication price (a) set at 10% of the diesel fuel price assumed to correlate perfectly with diesel fuel price, van capacity (m) of 27.22 t, and biomass moisture content (w) of 0.3 (Anderson 2011).

2.4. Management scenarios for the case study area

A 10-year management simulation was conducted to estimate delivered feedstock volume and costs under current site-specific management objectives. The annual treatment area constraint was set according to management planning documents developed by the US Forest Service and UPCRP. Stocking-based prescriptions were constrained to 850 ha·year^{-1}, aspen regeneration prescriptions were constrained to 587 ha·year^{-1}, and pine restoration prescriptions were constrained to 445 ha·year^{-1}, totaling to 1882 ha·year^{-1}. The year that a given stand gets treated depends on the order in which the stands are selected for treatment (defined in the silvicultural prescription) and the annual treatment area constraint for that prescription. Once a unit is selected for treatment, it is no longer considered a candidate treatment unit for the duration of the simulation. The annual delivered volumes and costs are calculated for each species group (silvicultural prescription).

A second scenario was carried out to evaluate how treatment area (total area treated during the next 10 years) affects the quantity of treatment residue volume and the spatial distribution of treatments. The purpose of this analysis is to identify the capacity of the landscape in terms of feedstock supply and characterize how delivered costs change as allowable treatment area increases. Starting with proportion of the area treated in the first scenario, which is approximately 50% of the total candidate area, the treated area was increased iteratively by 10% until 100% of the candidate treatment area was selected for treatment. The area allocations to the prescriptions described in the current management scenario were proportionally consistent for each 10% augmentation. Total available residues were calculated for each 10% increase in allowable treatment area.

An additional analysis was performed to locate residues available at or below a specified delivered cost using a cost-dependent classification scheme. Delivered costs were calculated for each candidate treatment unit and categorized into \$5 increments. The available residues were summed for each delivered-cost category. From a market perspective, the assumption in this analysis is that residues generated from treatment would be supplied to end users at a market price at or above the specified delivered cost, but that residues with higher costs would probably be burned in place for disposal because utilization would represent higher net costs than disposal.

3. Results and discussion

3.1. Stand delineation and characteristics

Stand boundaries were assessed by visual evaluation, compliance with the size restrictions, and the overall shape compactness value. The visual assessment consisted of scanning all stand boundaries superimposed on the NAIP imagery and checking for delineations that were incongruent with vegetation patterns observed in the imagery. Manual alterations of the stand boundaries were not necessary. Some of the boundaries separated apparently homogeneous and contiguous areas of forest cover. This is a result of the maximum stand area restriction and the algorithm's ability to numerically discriminate areas that might not be easily distinguishable by the human eye. This visual assessment was carried out only to identify any unexpected errors in the algorithm and to help fine tune algorithm parameters during the testing phase. The authors feel that visual assessment of all stand boundaries will not be necessary if the SDA is implemented on similar landscapes. However, if the SDA is used in a forest that is dissimilar in composition and structure than that of the present study site, then visual assessment is recommended.

The mean size of the delineated stands was 9.2 ha (SD = 10.3). All stands met the minimum and maximum size restrictions, with a minimum size of 2.95 ha and a maximum of 39.97 ha. The mean shape compactness value was 0.49 (SD = 0.14), with a maximum value of 0.89 and a minimum value of 0.11. In many cases, compactness values less than 0.2 were a result of the segmentation algorithm following roads and streams, yielding elongated shapes with poor compactness values. Buffering roads and streams prior to carrying out segmentation would likely resolve this issue and increase the mean compactness value.

The distribution of cover types across the UPNF is shown in Fig. 3. Cover types including scrub-oak, mountain mahogany, and other species cover 25.5% of the plateau. Mixed-conifer had the

Fig. 3. Mapped forest types across the study area. Enlarged areas show stand boundaries superimposed on NAIP CIR imagery and their respective forest type.

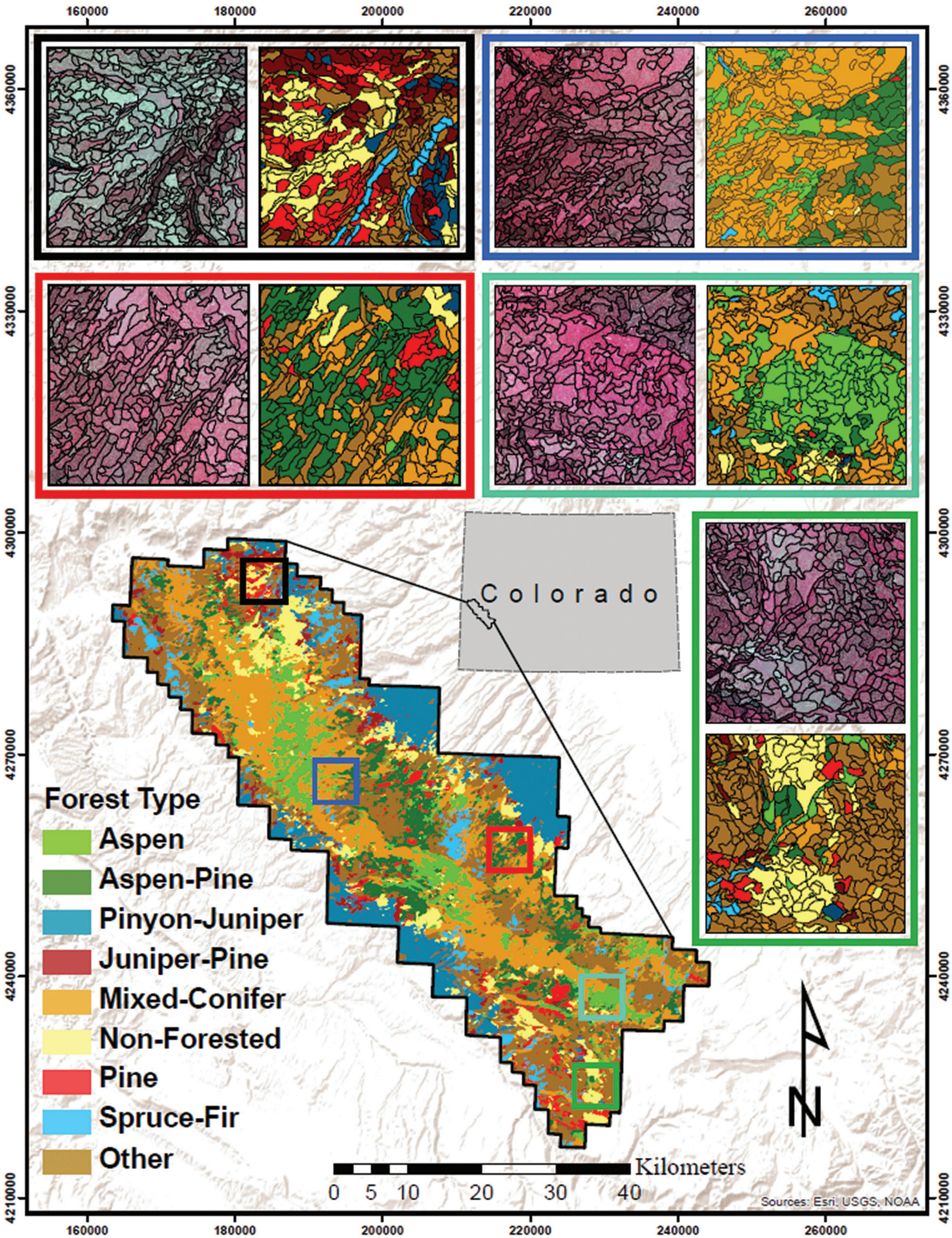

Table 1. Summary of forest characteristics by forest type.

Forest type	No. of stands	Area (ha)	BA ($m^2 \cdot ha^{-1}$)	Density (stems$\cdot ha^{-1}$)	QMD (cm)	AGB ($t \cdot ha^{-1}$)
Aspen	2123	19 866	22.96 (9.83)	444.79 (192.67)	25.40 (0.74)	48.99 (21.17)
Aspen–pine	3015	26 852	16.76 (6.45)	276.76 (124.96)	27.94 (1.75)	35.38 (14.16)
Pinyon–juniper	3266	30 121	14.69 (6.26)	143.32 (68.5)	35.56 (3.46)	15.42 (6.25)
Juniper–pine	950	8 768	10.56 (3.79)	111.20 (49.15)	35.56 (3.81)	15.42 (5.59)
Mixed conifer	5385	52 717	25.48 (10.69)	509.04 (210.12)	25.40 (0.89)	53.52 (22.63)
Pine	1033	8 340	9.41 (2.84)	108.73 (45.79)	33.02 (3.94)	19.05 (6.72)
Spruce–fir	1060	9 069	26.86 (12.28)	536.22 (234.78)	25.40 (1.27)	53.52 (25.79)
Other	6764	59 964	18.14 (8.76)	318.77 (176.81)	27.94 (2.39)	30.84 (18.87)
Nonforested	1943	19 142	—	—	—	—

Note: Values for basal area (BA), density, and aboveground biomass (AGB) represent the mean within the forest type (standard deviation in parentheses). QMD, quadratic mean diameter.

Fig. 4. Candidate treatment units by silvicultural prescription: (*a*) stocking-based management; (*b*) regeneration management; (*c*) restoration in ponderosa pine.

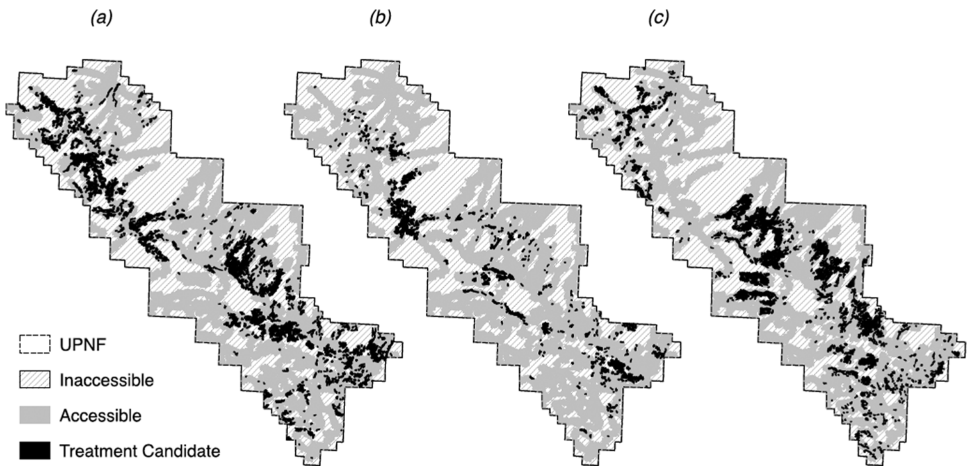

second highest coverage of 22.4%. Pinyon–Juniper occupies 12.8% of the plateau, covering mostly the lower elevations on the eastern and western extents. Pure aspen stands occur on the higher elevations, covering approximately 8.5% of the plateau. Ponderosa pine, spruce–fir, and other mixed-species (pine–juniper, aspen–pine) stands cover the rest of the forested area, and nonforested areas account for approximately 8% of the landscape. The values in Table 1 represent stand statistics for forest types across the study area. Forest types not assigned to a silvicultural prescription in treatment simulations are included to demonstrate the utility of the SDA and the FCM, which were conducted for the entire study area.

3.2. Silvicultural prescriptions

The selection of accessible forest stands resulted in 13 887 stands of the total 25 538 or 54% of the total area. A total of 5297 stands within the accessible area were considered candidate treatment units. The remaining accessible stands were given a "no treatment" prescription because they (*i*) currently meet desired future conditions, (*ii*) are in early seral stage, or (*iii*) are composed of a species group that is either not targeted or has high biomass logistical costs. The location of candidate treatment units by silvicultural prescription is shown in Fig. 4. These stands totaled to 46 840 ha, with 20 228 ha, 8102 ha, and 18 510 ha in stocking-based, regeneration, and restoration prescriptions, respectively.

3.3. Feedstock volume and delivered costs

Operations costs were calculated for all accessible stands across the study area. These costs represent handling, processing, and loading costs plus round-trip transportation costs to the bioenergy facility. Operations costs were close to normally distributed and ranged from $34.77·t^{-1}$ to $51.13·t^{-1}$, with a mean of $42.57·t^{-1}$ (SD = 3.28). These costs correlate perfectly with travel distance to the bioenergy facility as in-woods operations costs were fixed.

3.3.1. Current management

The 10-year management simulation resulted in 18 564 treated ha and 463 726 t of available treatment residue. The area treated is less than the constraint (18 820 ha), because when a stand is selected for treatment, the entire stand must be treated, not just a portion of the stand. The distribution of selected treatment stands for each simulated year is illustrated in Fig. 5. The distribution of delivered costs for each year is shown in Fig. 6. Year 6 had the largest range of delivered costs of $34.18 to $50.91·t^{-1}$. The lowest mean delivered cost was $42.02·t^{-1}$ during year 2 and the highest was during year 10 at $42.98·t^{-1}$. The mean delivered cost for the 10-year simulation was $42.54·t^{-1}$ (SD = 3.24).

Although the area constraints were held constant throughout the simulation, the available residue decreased each year (Table 2). This was a result of treatment prioritization targeting higher stocked stands in the beginning of the simulation. It is worth noting that this decreasing trend is likely to persist if the simulation is continued for a longer planning horizon. This is in part due to the absence of forest growth in the presented methodology as understocked stands may grow into overstocked stands during the 10-year planning horizon, but it is primarily attributable to the treatment prioritization schemes that were based on ecological goals: restorative management regimes targeted at overstocked stands tend to produce large amounts of treatment residue including nonmerchantable small-diameter trees. The long-term management goal of restoration means that more hectares of forest will be changed from current overstocked conditions to a state that more closely represents historic reference

Fig. 5. Stands selected for treatment by simulation year are indicated in black, and stands treated in previous years are indicated in grey.

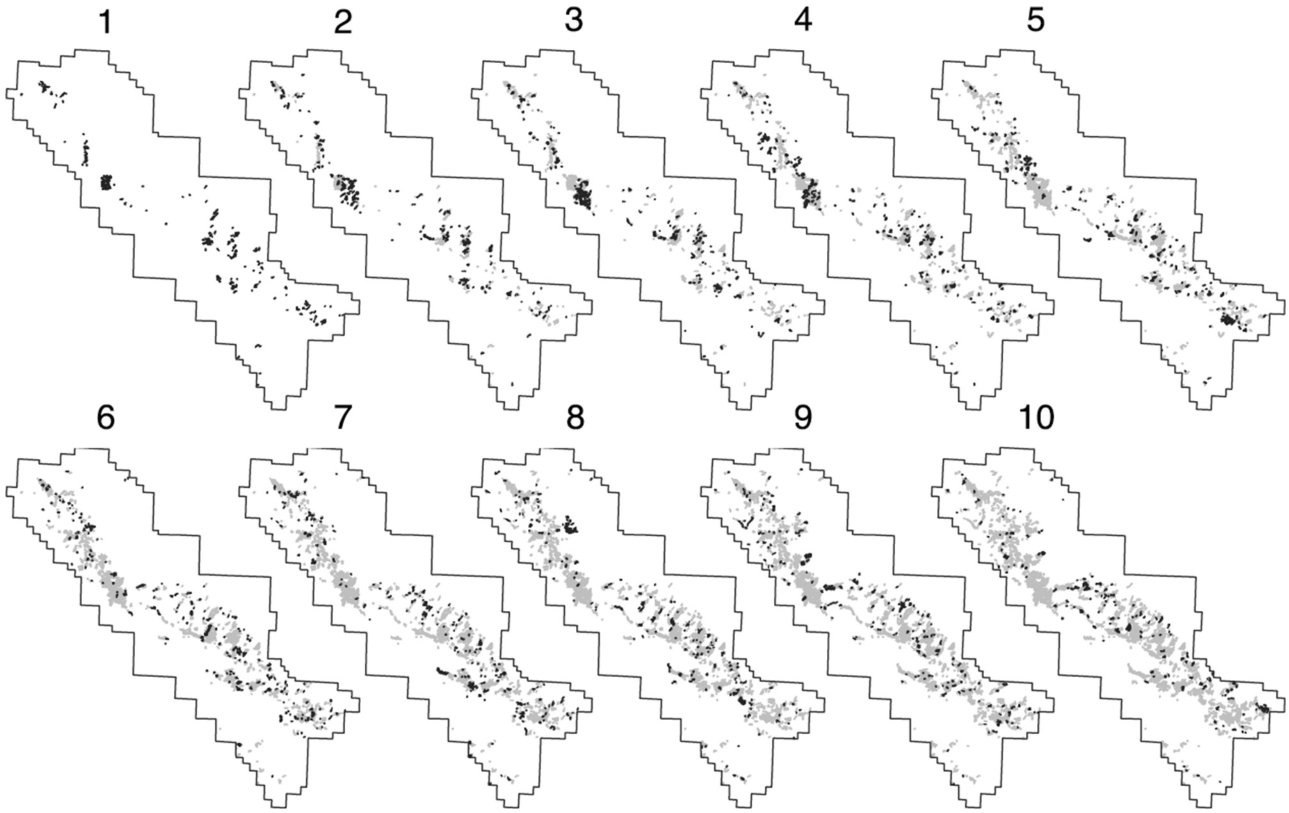

Fig. 6. Distribution of operations costs per year. Black lines represent the median costs and points represent mean costs.

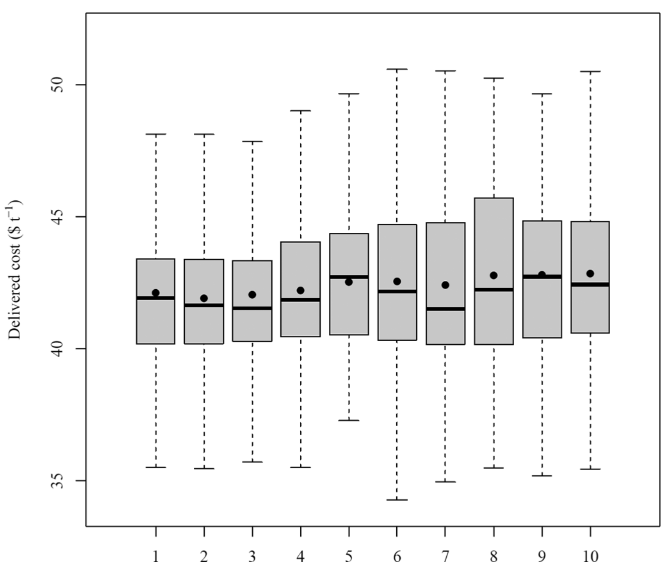

Table 2. Summary of pretreatment aboveground biomass (AGB), removed biomass, merchantable yield, treatment residue, and available feedstock per year over the 10-year management simulation.

Year	Area (ha)	AGB (t)	Removed biomass (t)	Merchantable yield (t)	Treatment residue (t)	Feedstock (t)
1	1861	392 094	193 936	111 920	73 851	51 696
2	1827	354 698	191 892	118 271	73 060	51 142
3	1870	337 680	184 988	114 928	70 060	49 042
4	1832	317 217	178 740	111 020	67 721	47 405
5	1874	311 540	181 018	112 418	68 600	48 019
6	1867	294 931	174 710	108 690	66 021	46 215
7	1874	277 972	166 400	103 139	62 355	43 648
8	1867	265 062	160 152	99 956	60 195	42 137
9	1836	257 877	160 792	100 170	60 622	42 434
10	1856	239 137	158 033	98 050	59 983	41 988

Table 3. Proportion of area and aboveground biomass (AGB) in accessible, candidate, and treated units to the total study area (landscape).

Selection area	Area (ha)	AGB (t)	% of total area	% of total AGB	AGB ($t \cdot ha^{-1}$)
Landscape	234 842	20 126 839	100	100	86
Accessible	126 495	10 735 459	54	53	85
Candidate	46 839	5 936 051	20	30	128
Treated	18 564	3 048 209	8	15	166

conditions, especially if periodic low-intensity natural and prescribed fires are used as a management tool to maintain understory conditions where appropriate. It is expected that available residue volumes will continue to decrease as the forests approach the desired future conditions. Note that the stands selected for treatments account for only 8% of the total area, while the aboveground biomass in these stands accounts for 15% of the total (Table 3). In theory, available residue will stabilize, assuming that management intensity (treatment area constraints) remains constant and restoration efforts involve natural mechanisms such as fire to maintain historic stand densities and structure.

From a biomass supply perspective, it is important to recognize that restoration treatments differ from even-aged silviculture for timber management, which includes periodic overstory removal to harvest mature timber and regenerate the stand, and are capable of supplying a sustained yield of biomass residues associated

Fig. 7. Available residue volume by silvicultural prescription at each simulated treatment level.

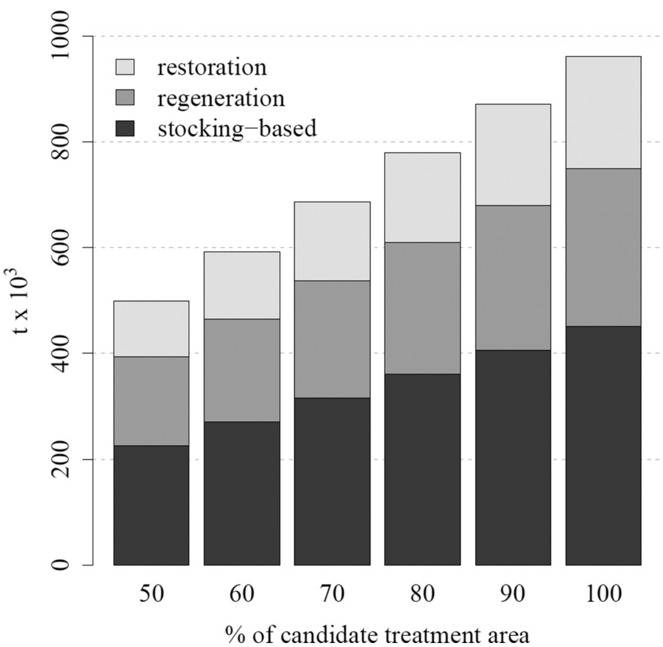

Fig. 8. Change in distribution of treatments as allowable treatment area restriction increases. Stands selected at 50% allowable treatment area are indicated in black, and stands selected at 100% allowable treatment area are indicated in grey.

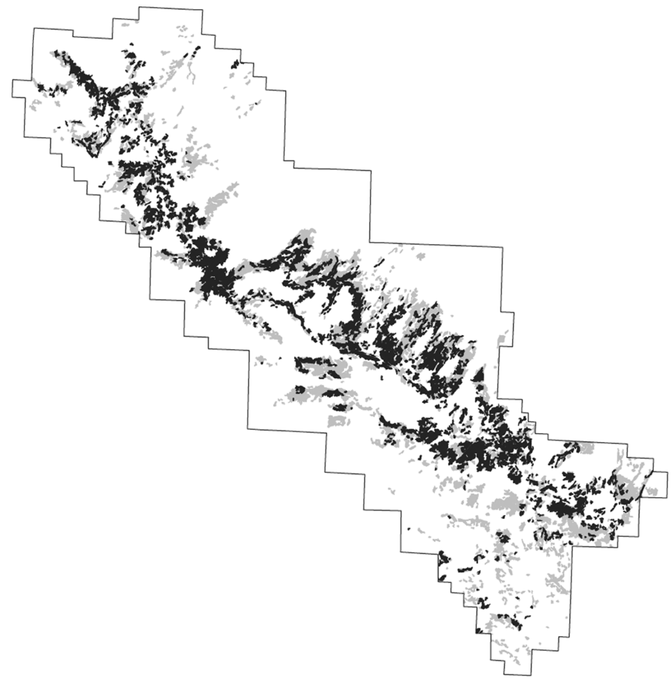

with timber harvest. We would not expect such a decline in available residues in an even-aged timber management context.

3.3.2. Augmented allowable treatment area

The augmented treatment area simulation resulted in a linear increase in treatment residue from 499 735 t to 960 905 t at 50% and 100% of candidate treatment area, respectively. The 50% allowable treatment area was considered the base case condition because the area treated was similar to that of the current management scenario. Each 10% increase in allowable treatment area added approximately 9000 t of available treatment residue. Conceivably, the proportion of residue in each silvicultural designation remains roughly consistent during each 10% increase in allowable treatment area (Fig. 7). The mean annual available treatment residue was 49 974 t·year^{-1} (SD = 3854) at 50% treatment area and culminated at 100% yielding 96 091 t·year^{-1} (SD = 5415) of residue. The spatial distribution of residues in this scenario was similar to that of the current management scenario, thus the delivered cost per tonne, which hinges on transportation cost, remains relatively consistent during each 10% increase in treatment area. The mean delivered cost for all treatment area augmentations was \$41.89·t^{-1} (SD = 3.43). The location of stands selected at 50% (black) and 100% (gray) allowable treatment area is shown in Fig. 8.

Stocking-based management was assigned to the mixed-conifer and spruce–fir species groups and accounted for the largest percentage (43%) of the total candidate treatment area. Therefore, the stocking-based prescriptions produce the largest percentage of available residue at all treatment levels. Conversely, stands selected for regeneration management, only 20% of the candidate treatment area, produced the second largest percentage of total available residue. This was due to the removal of all growing stock in these stands. Although restoration treatments in ponderosa pine covered 40% of the candidate treatment area, these stands produced the lowest residue volumes at all treatment levels due to low pretreatment basal area values relative to mixed-conifer, spruce–fir, and aspen stands.

It is likely that the establishment of a bioenergy supply chain will provide incentives to increase the allowable treatment area. According to these results, it is estimated that each 10% increase (from 50% to 100%) in allowable treatment area will yield 9000 t of feedstock without significantly increasing or decreasing delivered costs. This relationship might not be consistent if this analysis is repeated on a managed forest operating at an annual allowable treatment level that is large in proportion to the candidate treatment area. Furthermore, in certain situations, increasing the allowable treatment area can have negative impacts on mean delivered costs if more treatments are scheduled further away from the bioenergy facility.

3.3.3. Economic classification of candidate treatment area

The spatial structure of delivered costs for residues across the candidate treatment area is shown in Fig. 9. Nearly 55% (524 154 t) of the residues within the candidate treatment area are available at \$40–\$45·t^{-1}, and roughly 33% (321 812 t) of residues are available at \$45–\$50·t^{-1} (Table 4). These results can be used to prioritize treatments early in the development of a bioenergy supply chain to initiate markets by allocating efforts to residues available at relatively low costs. As markets develop, managers can begin to incorporate the acreage allocation constraints to meet forest-wide desired future conditions. Potential end users can use this information to evaluate feedstock prices that would result in different levels of feedstock supply and production.

In certain forests, the primary management focus is to improve forest health using restoration treatments. Commonly, these treatments produce a large amount of low-grade materials with high logistical costs and low market value. Existing markets are typically dominated by fuel markets for electricity production and co-generation of heat and power by forest industry facilities, sometimes with emerging demand by pellet mills and smaller bioenergy and bioproducts facilities. For the UPNF, where 70% of the forest is in fire regime condition class 2 or 3 and markets are very limited, a strategic approach to biomass analysis can support emerging biomass markets in several ways.

In other situations such as commercial forests in which broad-scale restoration is not a primary concern, different strategies may be more appropriate. Nonetheless, this methodology was

Fig. 9. Spatial distribution of delivered costs for the candidate treatment area. Delivered costs are categorized in $5 increments.

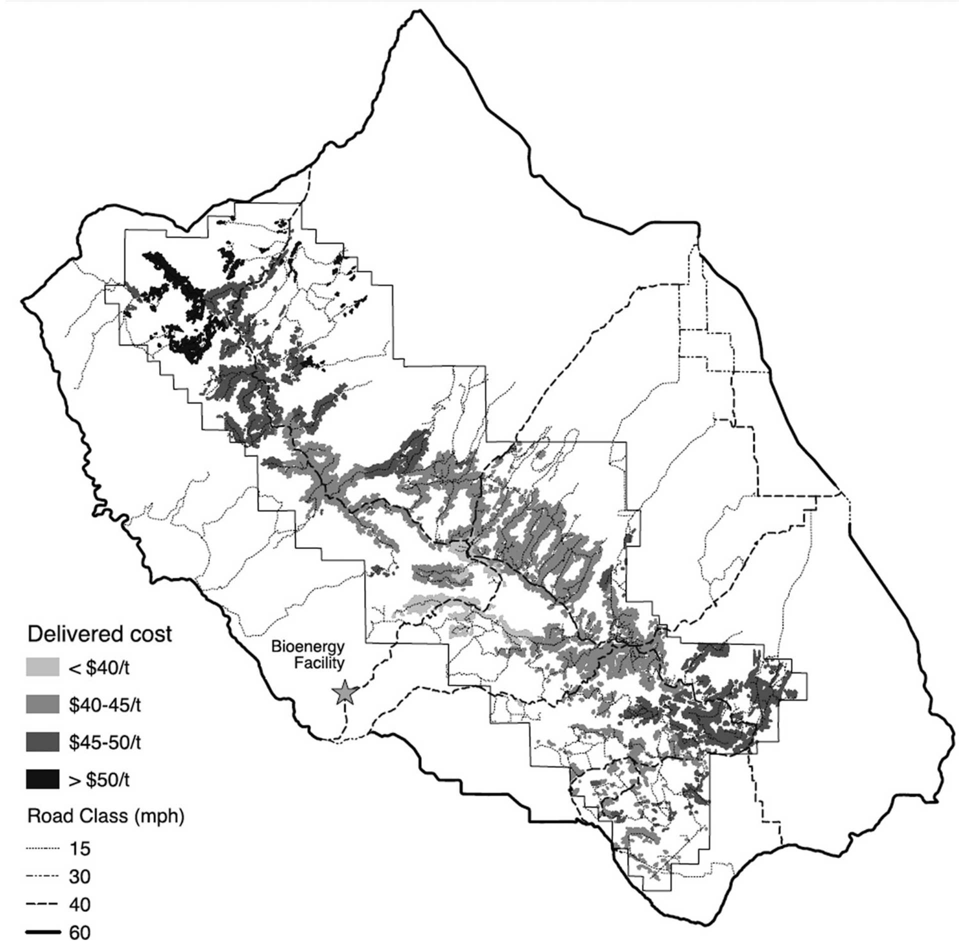

Table 4. Area treated and treatment residue for each delivered-cost category.

Delivered cost ($· t^{-1})	Area (ha)	Residue (t)	Cumulative residue (t)
<40	3153	56 924	56 924
40–45	25 627	524 154	581 078
45–50	14 915	321 812	902 890
>50	3144	58 015	960 906

designed with adaptability in mind to accommodate a range of management objectives across a diversity of landscapes and resources. The NAIP and FIA datasets used in this study have broad national coverage, facilitating similar analysis throughout the US, but any similar remote sensing and inventory data can be used.

4. Conclusion

The integration of the stand delineation algorithm and the FCM, coupled with site-specific silvicultural prescriptions and operational planning, presents the opportunity to carry out detailed spatial analysis for a diversity of resources on very large landscapes. As demonstrated in this study, the methodology can be employed to assess the feasibility of biomass utilization, assist silvicultural decisions, and facilitate operational planning at tactical and operational scales. The capacity to not only estimate residue quantities but also to map the spatial distribution of stand-level residues following alternative management regimes is vital in areas with limited history of industrial biomass utilization and uncertainties in biomass markets. This information is useful to stakeholders across the biomass supply chain, including land managers, contractors, and end users.

Research is still needed to fill the knowledge gap regarding residue leakage from stump to landing and recovery rates at the landing, as well as site-specific forest operations costs. Small changes in leakage and recovery rates can drastically influence estimated biomass availability. Although this study assumed a 70% reduction rate to account for stump-to-landing leakage and recovery at the landing, this can vary significantly depending on species, time since harvest, level of stand mortality, and other variables. An improved model would incorporate forest growth in temporal simulation, allowing more accurate estimates well beyond the 10-year time frame used in this study. This improvement would broaden the planning horizon to better understand the sustainability of biomass flows, as well as the long-term viability of supplying bioenergy and biofuels facilities with biomass from forest restoration treatments. The assumption that the road network will remain static over the next 10 years may result in significant underestimation of potential supply volume. It is recommended that proposed road additions are included or proposed road decommissions are excluded in the presented workflow to deal with changes in accessibility. Future studies could use this methodology to optimally locate bioenergy facilities in the region in ways to reduce feedstock procurement costs and determine the scale at which they could operate sustainably and in balance with forest management regimes that meet a broad range of social, economic, and ecological objectives.

Acknowledgements

This research was supported by the Agriculture and Food Research Initiative, Biomass Research and Development Initiative

(Competitive Grant No. 2011-10006-30357) from the USDA National Institute of Food and Agriculture and a USFS Rocky Mountain Research Station Grant (No. 10-JV-11221636-282) with significant cost match and in-kind support from the University of Montana and Oregon State University.

References

Abbas, D., Current, D., Phillips, M., Rossman, R., Hoganson, H., and Brooks, K.N. 2011. Guidelines for harvesting forest biomass for energy: a synthesis of environmental considerations. Biomass Bioenergy, **35**: 4538–4546. doi:10.1016/j.biombioe.2011.06.029.

Anderson, N.M. 2011. Estimating the delivered costs of biomass from the Uncompahgre Plateau using Monte Carlo simulation. A mid-project summary. Prep. stakeholders, partners Cooperative Rocky Mountain Research Station Competitive Research Initiative – Uncompahgre Plateau Project.

American Transportation Research Institute (ATRI). 2013. American Truck Associations Federation. Available from http://atri-online.org/. [Accessed 11 October 2013.]

Baral, A., and Guha, S. 2004. Trees for carbon sequestration or fossil fuel substitution: the issue of cost vs. carbon benefit. Biomass Bioenergy, **27**: 41–55. doi:10.1016/j.biombioe.2003.11.004.

Beven, K.J., and Kirkby, M.J. 1979. A physically based, variable contributing area model of basin hydrology. Hydrol. Sci. Bull. **24**: 43–69. doi:10.1080/02626667909491834.

Binkley, D., Romme, B., and Cheng, T. 2008. Historical forest structure on the Uncompahgre Plateau: informing restoration prescriptions for mountainside stewardship. Prepared by the Colorado Forest Restoration Institute, Colorado.

Brown, R.T., Agee, J.K., and Franklin, J.F. 2004. Forest restoration and fire: principles in the context of place. Conserv. Biol. **18**: 903–912. doi:10.1111/j.1523-1739.2004.521_1.x.

Burt, T., and Butcher, D. 1986. Stimulation from simulation? a teaching model of hillslope hydrology for use on microcomputers. J. Geogr. High. Educ. **10**: 23–39. doi:10.1080/03098268608708953.

Chung, W., and Sessions, J. 2003. NETWORK 2000, a program for optimizing large fixed and variable cost transportation systems. *In* Proceedings of the 8th Symposium on System Analysis in Forest Resources, Snowmass Village, Colorado, U.S.A. pp. 109–120. doi:10.1007/978-94-017-0307-9_12.

Daly, C., Gibson, W., Doggett, M., Smith, J., and Taylor, G. 2009. Near-real-time monthly high-resolution climate data set for the conterminous United States. Spatial Climate Analysis Service, Oregon State University, Corvallis, Oregon.

Fight, R.D., Hartsough, B.R., and Noordijk, P. 2006. Users guide for FRCS: fuel reduction cost simulator software. USDA Forest Service, Pacific Northwest Research Station, General Technical Report PNW-GTR-668. pp. 1–30.

Fukunaga, K., and Hostetler, L. 1975. The estimation of the gradient of a density function, with applications in pattern recognition. IEEE Trans. Inf. Theory, **21**: 32–40. doi:10.1109/TIT.1975.1055330.

Gan, J., and Smith, C.T. 2007. Co-benefits of utilizing logging residues for bioenergy production: the case for East Texas, USA. Biomass Bioenergy, **31**: 623–630. doi:10.1016/j.biombioe.2007.06.027.

Guo, Z., Sun, C., and Grebner, D.L. 2007. Utilization of forest derived biomass for energy production in the U.S.A.: status, challenges, and public policies. Int. For. Rev. **9**: 748–758. doi:10.1505/ifor.9.3.748.

Han, H.S., Halbrook, J., Pan, F., and Salazar, L. 2010. Economic evaluation of a roll-off trucking system removing forest biomass resulting from shaded fuelbreak treatments. Biomass Bioenergy, **34**: 1006–1016. doi:10.1016/j.biombioe.2010.02.009.

Hardy, C.C., Schmidt, K.M., Menakis, J.P., and Neil, S.R. 2001. Spatial data for national fire planning and fuel management. Int. J. Wildl. Fire, **10**: 353–372.

Helms, J.A. 1998. The dictionary of forestry. Society of American Foresters, Bethesda, Maryland.

Hogg, E.H. 1997. Temporal scaling of moisture and the forest–grassland boundary in western Canada. Agric. For. Meteorol. **84**: 115–122. doi:10.1016/S0168-1923(96)02380-5.

Hogland, J., Billor, N., and Anderson, N.M. 2013. Comparison of standard maximum likelihood classification and polytomous logistic regression used in remote sensing. Eur. J. Remote Sens. **46**: 623–640. doi:10.5721/EuJRS20134637.

Hogland, J.S., Anderson, N.M., Chung, W., and Wells, L. 2014. Estimating forest characteristics using NAIP imagery and ArcObjects. *In* Proceedings of the 2014 ESRI Users Conference, 14–18 July 2014, San Diego, California. Environmental Systems Research Institute, Redlands, California. pp. 1–22. Available from http://proceedings.esri.com/library/userconf/proc14/papers/155_181.pdf.

Jenkins, J.C., Chojnacky, D.C., Heath, L.S., and Birdsey, R.A. 2003. National-scale biomass estimators for United States tree species. For. Sci. **49**: 12–35.

Jones, G., Loeffler, D., Calkin, D., and Chung, W. 2010. Forest treatment residues for thermal energy compared with disposal by onsite burning: emissions and energy return. Biomass Bioenergy, **34**: 737–746. doi:10.1016/j.biombioe.2010.01.016.

Loeffler, D., and Anderson, N.M. 2014. Emissions tradeoffs associated with cofiring forest biomass with coal: a case study in Colorado, USA. Appl. Energy, **113**: 67–77. doi:10.1016/j.apenergy.2013.07.011.

Moore, I.D., Grayson, R.B., and Ladson, A.R. 1991. Digital terrain modeling: a review of hydrological geomorphological and biological applications. Hydrol. Process. **5**: 3–30. doi:10.1002/hyp.3360050103.

Puttock, G.D. 1995. Estimating cost for integrated harvesting and related forest management activities. Biomass Bioenergy, **8**: 73–79. doi:10.1016/0961-9534(95)00001-N.

Reineke, L.H. 1933. Perfecting a stand-density index for even-aged forests. J. Agric. Res. **46**: 627–638.

Rodhe, A., and Seibert, J. 1999. Wetland occurrence in relation to topography: a test of topographic indices as moisture indicators. Agric. For. Meteorol. **98–99**: 325–340. doi:10.1016/S0168-1923(99)00104-5.

Rummer, B., Prestemon, J., May, D., Miles, P., Vissage, J., McRoberts, R., Liknes, G., Shepperd, W.D., Ferguson, D., Elliot, W., Miller, S., Reutebuch, S., Barbour, J., Fried, J., Stokes, B., Bilek, E., and Skog, K. 2003. A strategic assessment of forest biomass and fuel reduction treatments in Western States. USDA Forest Service, Research and Development. Available from http://www.treesearch.fs.fed.us/pubs/23846.

Schmidt, K.M., Menakis, J.P., Hardy, C.C., Hann, W.J., and Bunnell, D.L. 2002. Development of coarse-scale spatial data for wildland fire and fuel management. USDA Forest Service, Gen. Tech. Rep. RMRS-GTR-62.

Seibert, J., Bishop, K.H., and Nyberg, L. 1997. A test of TOPMODEL's ability to predict spatially distributed groundwater levels. Hydrol. Process. **11**: 1131–1144. doi:10.1002/(SICI)1099-1085(199707)11:9<1131::AID-HYP549>3.3.CO;2-R.

Shields, W.J., Jr., and Bockheim, J.G. 1981. Deterioration of trembling aspen clones in the Great Lakes region. Can. J. For. Res. **11**(3): 530–537. doi:10.1139/x81-073.

USDA Farm Service Agency. 2011. National agricultural imagery program. USDA Farm Service Agency, Aerial Photography Field Office, Salt Lake City, Utah.

USDA Forest Service. 2012. Grand Mesa Uncompahgre and Gunnison National Forests. Current Forest Plan. Available from http://www.fs.usda.gov/detail/gmug/landmanagement/planning/?cid=fsbdev7_003229. [Accessed 20 September 2013.]

U.S. Department of Energy. 2011. US billion-ton update: biomass supply for a bioenergy and bioproducts industry. Oak Ridge National Laboratory, Oakridge, Tennessee.

U.S. Geological Survey (USGS). 2006. Watershed boundary data — 12 digit hydrological units. Available from http://www.nrcs.usda.gov/wps/portal/nrcs/main/national/water/watersheds/dataset/.

Wells, L.A. 2013. Spatial distribution and quantification of forest treatment residues for bioenergy production. M.Sc. thesis, University of Montana, College of Forestry and Conservation. Available from http//scholarworks.umt.edu/etd/4177.

Worrall, J.J., Egeland, L., Eager, T., Mask, R.A., Johnson, E.W., Kemp, P.A., and Shepperd, W.D. 2008. Rapid mortality of *Populus tremuloides* in southwestern Colorado, U.S.A. For. Ecol. Manage. **255**: 686–696. doi:10.1016/j.foreco.2007.09.071.

Worrall, J.J., Marchetti, S.B., Egeland, L., Mask, R.A., Eager, T., and Howell, B. 2010. Effects and etiology of sudden aspen decline in southwestern Colorado, U.S.A. For. Ecol. Manage. **260**: 638–648. doi:10.1016/j.foreco.2010.05.020.

Zhang, L., Bi, H., Gove, J.H., and Heath, L.S. 2005. A comparison of alternative methods for estimating the self-thinning boundary line. Can. J. For. Res. **35**(6): 1507–1514. doi:10.1139/x05-070.

Zinko, U., Seibert, J., Dynesius, M., and Nilsson, C. 2005. Plant species numbers predicted by a topography-based groundwater flow index. Ecosystems, **8**: 430–441. doi:10.1007/s10021-003-0125-0.